# Predictions for the SKA from hierarchical galaxy formation models

C. M. Baugh[a] *, C. G. Lacey[a], C. S. Frenk[a], A. J. Benson[b], S. Cole[a], G. L. Granato[c], L. Silva[d], A. Bressan[c].

[a]Institute for Computational Cosmology, Department of Physics,
University of Durham, South Road, Durham, DH1 3LE.

[b]Astrophysics, University of Oxford, Keble Road, Oxford.

[c]Osservatorio Astronomico di Padova, Vicolo dell'Osservatorio, 5, I-35122 Padova, Italy.

[d]Osservatorio Astronomico di Trieste, via Tiepolo 11, I34131 Trieste, Italy.

There is now overwhelming evidence to suggest that structure in the Universe formed hierarchically. The development of collapsed structures in the dark matter due to gravitational instability has been studied extensively using numerical simulations and analytic techniques. Modelling the baryonic component of the Universe is much more challenging. The process of galaxy formation and evolution can be followed in the context of hierarchical structure formation using the technique of semi-analytical modelling. Due to our lack of knowledge of the pertinent physics, some parts of the model are more uncertain than others, one clear example being the parameterization of the timescale for star formation. The SKA will help to remove this ambiguity by testing predictions for the evolution of the distribution of star formation rates and the neutral hydrogen mass function. Here we give examples of such predictions for two models which differ in how the star formation timescale in galaxies scales with redshift. We use the `GALFORM` semi-analytical model to compute the evolution of the neutral hydrogen mass function with redshift. The star formation histories generated by the `GALFORM` model are combined with the spectro-photometric code `GRASIL` to generate spectral energy distributions for model galaxies that extend beyond the optical to sub-millimetre and radio wavelengths. We use this hybrid code to make predictions for the number counts of radio sources whose radio emission is driven by star formation.

## 1. Simulating hierarchical galaxy formation

In the gravitational instability paradigm for the formation of cosmic structure, small density perturbations grow through the accretion of mass and by mergers. Within this framework, the variant of the cold dark matter (CDM) model with a cosmological constant, ΛCDM, has enjoyed remarkable success, most notably in providing an impressively faithful description of the pattern of microwave background temperature fluctuations (Spergel et al. 2003 [34]).

Numerical simulations of the hierarchical clustering of the dark matter reveal a cosmic web of filaments, voids and cluster-sized haloes that looks similar to the galaxy distribution, as mapped out locally by surveys such as the two-degree Field Galaxy Redshift Survey and the Sloan Digital Sky Survey (e.g. Peacock et al. 2001 [25]). Similar calculations can also model the detailed internal structure of dark matter haloes or trace the structures that may have hosted the first generation of stars in the Universe. However, to take the next step from a calculation of structure formation in the dark matter to produce a model that describes the formation of galaxies requires the physics of the baryonic component of the Universe to be considered.

Modelling the physics of the baryonic gas is a much more difficult task than following the dark matter by itself for two reasons. Firstly, the computational demands are greater, because the baryons tend to become more concentrated than the dark matter since they are able to radi-

*Research supported by PPARC and the Royal Society.

ate energy away. Secondly, many of the physical processes believed to be important in galaxy formation are simply poorly understood and therefore impossible to model without invoking recipes with parameters. Two approaches have been followed to overcome these difficulties: direct numerical simulations, that follow the gas dynamics using particles or refined meshes (e.g. Okamoto et al. 2003 [24], Quilis 2004 [28]) and semi-analytical modelling (e.g. Kauffmann, White & Guiderdoni 1993[21]; Cole et al. 1994 [8]; Somerville & Primack 1999 [33]). These two classes of model are more similar than is often realized and should be viewed as complementary. Whereas direct simulations avoid the need for simplifying specialized assumptions, semi-analytical models are faster and more flexible. Direct simulations always come up against processes that are beyond their resolution, termed "sub-grid" physics, e.g. in their implementation of star formation and the impact of supernovae explosions. When this limit is reached, direct simulations should really be thought of as having becoming "semi-analytical" models themselves.

In semi-analytical models, the physics of galaxy formation is encoded in a set of rules that are physically motivated, and, where possible, have been designed to mimic the results of numerical simulations e.g. the consequences of galaxy mergers of a particular mass ratio. A dark matter halo merger tree (its "family history") is produced using either Monte Carlo techniques or by extraction from an N-body simulation (see Helly et al. 2003a[15]). The uppermost branches of the tree are filled with gas that is shock heated to the virial temperature of these progenitor halos, and the set of rules is followed to describe the subsequent evolution of this gas.

Here we use the semi-analytical code `GALFORM`, which was introduced by Cole et al. (2000) [9], and has been augmented in a series of papers (Granato et al. 2000 [13]; Benson et al. 2002 [3]; Benson et al. 2003 [4]). The physical processes that are considered in this model are the following: (i) The hierarchical growth of dark matter haloes. (ii) The virialisation of gas within the gravitational potential wells of the dark matter haloes. (iii) The radiative cooling of gas onto a galactic disk. This may be suppressed in low circular velocity haloes due to the presence of a background of photoionizing radiation (Benson et al. 2002 [3]). (iv) The formation of stars from the cooled gas. (v) Reheating and expulsion of the cooled gas through feedback processes such as stellar winds and supernoave explosions (see Benson et al. 2003 [4]). (vi) The chemical evolution of the stars and gas. (vii) Mergers between dark matter haloes and galaxies. Galaxy mergers may be accompanied by bursts of star formation, depending on the violence of the merger (Baugh et al. 2004 [1]). Mergers may lead to the production of a galactic bulge. (viii) The calculation of the sizes of the disk and bulge components of model galaxies. (ix) The evolution of the stellar population of the galaxies through population synthesis models.

The parameters of the semi-analytical model are chosen by requiring that the model reproduces a subset of the observational data for the local galaxy population, such as the optical and near-infrared field luminosity functions (see Cole et al. 2000 [9]).

## 2. Modelling the accretion of cold gas

Recently there has been renewed interest in the means by which cold gas arrives in galaxies. In the semi-analytical model, as outlined above, we assume that the baryons are heated to the virial temperature of the dark matter halo by shocks produced during the collapse of the halo. A cooling time is computed for the hot gas, using a collisional cooling rate that depends upon the metallicity of the hot gas (Sutherland & Dopita 1993 [37]). This timescale is used to obtain a cooling radius within which gas has been able to cool during the lifetime of the halo. The cooling radius propagates outwards until either all the gas in the halo has cooled or a new dark halo forms; a shell of gas cools in each timestep. This cooled gas is accreted onto the disk of the galaxy on the freefall timescale. At high redshifts, the typical cooling times are very short and the rate at which cold gas arrives in the disk is set by the free fall time.

This calculation of the rate at which gas cools and is added to galactic disks is very idealised.

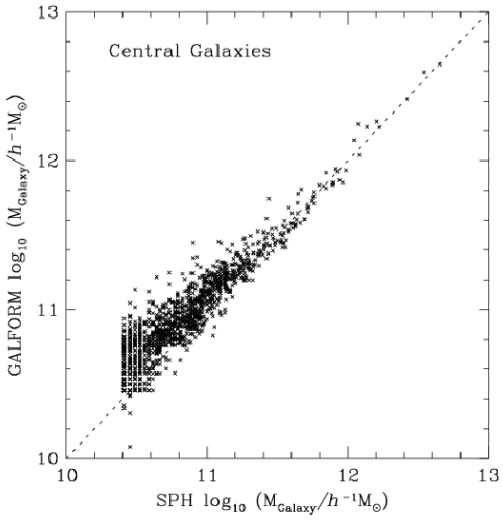


Figure 1. The mass of cold gas in the central or most massive galaxies in haloes taken from an N-body & SPH simulation. The mass of the central galaxy in the SPH calculation is compared with that predicted by a "stripped-down" version of the semi-analytic model, which uses the dark matter merger trees from the simulation. In both cases, star formation and feedback are switched off. (Adapted from Helly et al. 2003b.[16])

In particular, one could question the validity of two of the main assumptions underpinning the above model: (i) the gas is first shock heated to the virial temperature of the dark matter halo in all cases and (ii) a spherically symmetric cooling radius propagates steadily outwards. Analytical calculations and simulations suggest that for low mass haloes, shocks are ineffective in heating the gas (Katz et al. 2002 [20]; Birnboim & Dekel 2003[5]; Keres et al. 2004[22]). At high redshifts this may be of little relevance as the cooling times are so short that, in practice, it is the freefall time that limits the accretion of gas onto a galactic disk. Anyone who has seen pictures of a high resolution simulation of a dark matter halo will wonder as to how the assumption of spherical symmmetry can ever be a good description of the accretion of matter down filaments. Given these quite reasonable reservations, and since the cooling model lies at the heart of the galaxy formation process as it governs the supply of the raw material for star formation, it is clearly important to test how well these simple calculations reproduce what happens in simulations.

Several comparisons have been made between the distribution of cold gas predicted in "stripped down" semi-analytical models and direct smooth particle hydrodynamics (SPH) gas simulations (Benson et al. 2001 [2]; Yoshida et al. 2002 [39]; Helly et al. 2003b [16]). In these models, star formation and feedback are switched off to aid in the interpretation of the results. Helly et al. (2003b) [16] extracted dark matter halo merger trees from an N-body & SPH simulation, and used these in a stripped down semi-analytical model to compute the mass of gas that cooled. Fig. 1 compares the cold gas masses recovered from the two calculations for the central or most massive galaxies in dark matter haloes. The two approaches give reassuringly similar results for the mass of cold gas in well resolved haloes.

## 3. The models

We consider two models that differ in a number of ingredients. Both models assume the ΛCDM cosmology. The first model is the fiducial model of Cole et al. (2000)[9]. In this model, we adopted a baryon density parameter of $\Omega_b = 0.02$, which was compatible with the nucleosynthesis constraints at the time of writing Cole et al. Furthermore, the star formation timescale in this model scales in proportion to the dynamical time within a galaxy. This means that the typical star formation timescale gets shorter with increasing redshift. The second model is described in Baugh et al. (2004)[1]. In this case, $\Omega_b = 0.04$. To prevent too many luminous galaxies forming, a galactic superwind is invoked (see Benson et al. 2003 [4] for a discussion of how this phenonmenon is incoporated). The effects of a photoionising background are included by preventing any gas from cooling in haloes with circular velocity $< 60\mathrm{kms}^{-1}$ at $z < 6$. The star formation timescale does not scale with the dynamical time

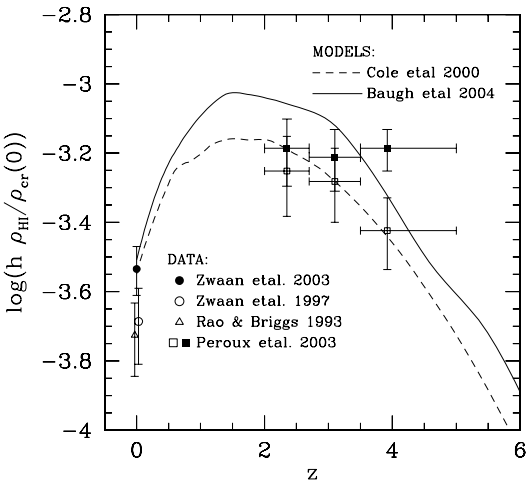


Figure 2. The mass density of HI, expressed in units of the present day critical density, as a function of redshift. The model predictions are shown by lines, as indicated by the key. At $z = 0$, several recent determinations of the neutral atomic hydrogen density are plotted (the open symbols have been offset in redshift for clarity). At high redshift, the open squares show the density of HI measured from damped Lyman-$\alpha$ systems by Peroux et al. (2003)[26]; the filled squares show these values after a correction for systems below the damped Lyma-$\alpha$ column density threshold.

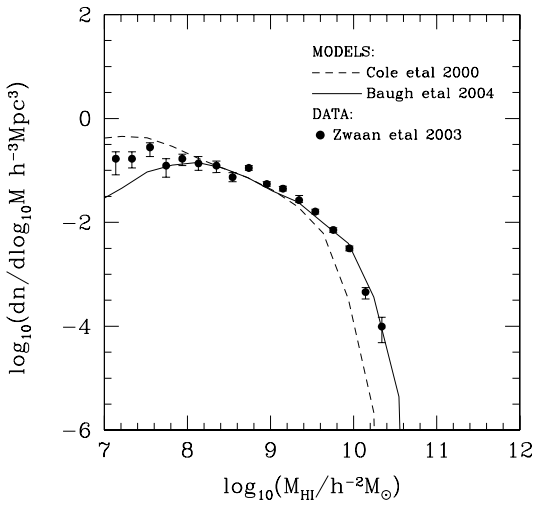


Figure 3. The HI mass function at $z = 0$. The points show the recent determination using HIPASS galaxies by Zwaan et al. (2003)[41]. The curves show the model predictions.

in this model, which means that galactic disks tend to be gas rich at high redshift. A consequence of this is that more star formation occurs in bursts triggered by galaxy mergers at high redshift. The stellar initial mass function (IMF) of stars formed in bursts is assumed to be flat in this model. Although this choice is controversial, Baugh et al. (2004) [1] show that using a flat IMF in bursts is a key facet of the new model, which is much more successful at reproducing the abundance of galaxies at high redshift – Lyman break galaxies and SCUBA detected sources – than was the case for the Cole et al. model. However, both models give very good matches to the local galaxy population.

## 4. The HI mass function

One of the main science drivers of the SKA is to map the distribution of neutral hydrogen in the Universe. `GALFORM` predicts the mass of cold gas in virialised dark matter haloes, allowing for sources (gas cooling, mergers) and sinks (star formation and reheating or ejection of cooled gas by feedback). The grid of halo masses that we simulate typically accounts for around 50% of the matter in the Universe (Jenkins et al. 2001[19]). The remaining baryonic mass, is assumed to be locked up in lower mass haloes ($< 10^{10} h^{-1} M_{\odot}$ at $z = 0$) in which star formation is very inefficient, with any gas that is able to cool reheated and ejected by supernova feedback.

We have taken the route of correcting the mass of cold gas predicted by the model to obtain the mass of HI to compare with the observations. The first step is to take into account that $\sim 24\%$ by mass of the gas is helium. Next, we need to account for the fraction of hydrogen that is in molecular rather than atomic form. Keres, Yun & Young (2003) [23] measured the luminosity of CO, which can be sim-

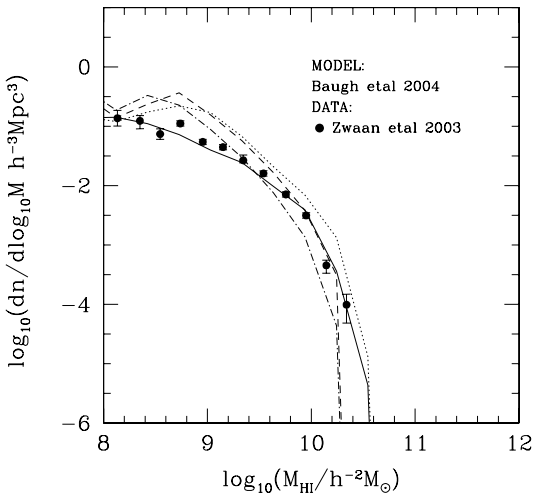


Figure 4. The evolution of the HI mass function with redshift in the Baugh et al. (2004) [1] model. The points show the recent $z = 0$ determination using HIPASS galaxies by Zwaan et al. (2003) [41]. The curves show the model predictions at different redshifts (solid: z=0 ; dotted: z=1 ; dashed: z=3, dot-dashed: z=4).

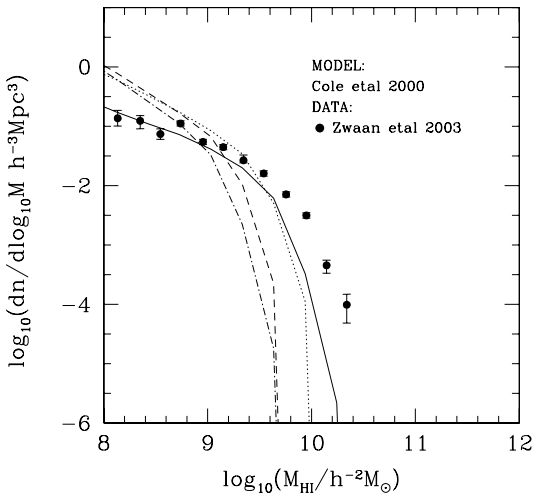


Figure 5. The evolution of the HI mass function with redshift in the Cole et al. (2000) [9] model. The points show Zwaan et al. (2003) [41] estimate of the mass function at $z = 0$. The line styles are the same as used in Fig. 4.

ply related to the mass of molecular hydrogen. Keres et al. estimate a density of molecular hydrogen of $\rho_{\rm H_2} = (3.1 \pm 0.9) \times 10^7 h M_\odot {\rm Mpc}^{-3}$ (note we use $H_0 = 100h{\rm kms}^{-1}{\rm Mpc}^{-1}$). If we use the mass density of neutral atomic hydrogen measured by Zwaan et al. (2003) [41], $\rho_{\rm HI} = (8.1 \pm 1.3) \times 10^7 h M_\odot {\rm Mpc}^{-3}$, then the fraction of mass in molecular compared with atomic hydrogen is 0.4. Note this is substantially lower than the value advised by Fukugita, Hogan & Peebles (1998) [12] and somewhat lower than advocated by Keres et al., due to the HI mass density measured by Zwaan et al. (2003) [41] being higher than previous estimates. Therefore, in the model we set $M_{\rm HI} = 0.76 M_{\rm cold}/(1 + 0.4)$.

We compare the predictions of the two theoretical models with observational estimates of the mass density of HI at different redshifts in Fig. 2. The model predictions, shown by the lines, differ from one another by at most a factor of 1.5 at high redshift and give essentially the same amount of HI at the present day. At $z = 0$, the models are required to match local observations of the gas to luminosity ratio in spiral galaxies, hence the similarity between the model predictions at this redshift. However, the models predict more mass than the earlier estimates HI estimates by Rao & Briggs (1993) [29] and Zwaan et al. (1997) [40]. The best current observational estimate is that by Zwaan et al. (2003) [41] using the 1000 brightest galaxies from the HIPASS survey. This is now in excellent agreement with the model predictions. At high redshift, we have plotted the HI density estimated by Peroux et al. (2003) [26], who used a new sample of damped Lyman-$\alpha$ absorbers and Lyman limit systems, augmented by data from the literature (Storrie-Lombardi et al. 1996 [35]; Storrie-Lombardi & Wolfe 2000 [36]). We have taken the $\Omega_{\rm DLA}$ from Table 1 of Peroux et al. and divided by the mean molecular mass, $\mu$, to get the HI mass. The filled points are taken from Fig. 6 of Peroux et al. and include a correction for systems below the column density of damped systems. The models bracket the inferred HI density and predict a peak in the density of neutral hydrogen around $z \sim 1 - 2$.

The predicted HI mass function is compared with the Zwaan et al. (2003) [41] determination in Fig. 3. The models agree reasonably well with the estimated mass function. The match above $M_{HI} = 10^8 h^{-2} M_\odot$ is particularly good for the new model; no model parameters were adjusted to achieve this level of agreement. The evolution of the HI mass function with redshift is presented in Fig. 4. The two flavours of the semi-analytical model predict quite different behaviour for the evolution of the HI mass function. There is relatively little evolution in the mass function in the case of the Baugh et al. model. This model predicts an increase in the number of objects with high HI masses to $z = 1$, then a gradual decline to $z = 4$, with a steepening in the low mass part of the mass function. On the other hand, Fig. 5 shows that the Cole et al. model predicts that the number of high HI mass objects declines with increasing redshift. This difference in the evolution is primarily driven by the different parameterisations of the star formation timescales employed in the two models.

## 5. Measuring the distribution of star formation rates

The SKA will be able to test the distribution of star formation rates predicted by hierarchical models by counting the number of faint radio sources. The SKA will probe the regime in which the radio emission from normal galaxies, due to the acceleration of electrons in supernovae and free-free emission in HII regions, begins to dominate over the counts due to galaxies whose emission is powered by accretion onto central supermassive black holes.

We compute the radio emission from normal star forming galaxies using the spectrophotometric code `GRASIL`, written by Silva et al. (1998)[32]. This code incorporates the simple models for the radio emission associated with star formation first put forward by Condon & Yin (1990) [10] and reviewed by Condon (1992) [11]. Bressan, Silva & Granato (2002) [6] used the `GRASIL` code to model the radio emission from dusty starbursts.

Here, we take the star formation histories predicted *ab initio* by `GALFORM` and feed these into the `GRASIL` code. The result is the spectral energy distribution of the galaxy, including the contributions from star formation, dust extinction, reradiation by dust and the acceleration of electrons in supernovae. The wavelength coverage of the SED stretches from the far-UV through the sub-millimetre to the radio. We present predictions from the model proposed by Baugh et al. (2004) [1] which reproduces the luminosity function of Lyman-break galaxies at $z = 3$ and the source counts of sources at $850\mu$m.

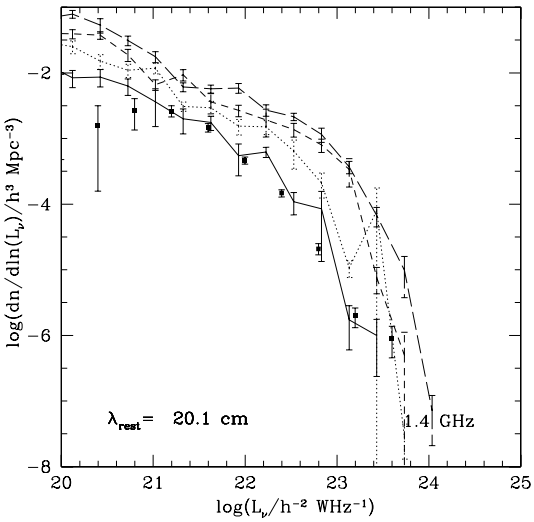


Figure 6. The 1.4 GHz luminosity function. The symbols show an observational estimate for local star forming galaxies by Sadler et al. (2002) [31]. These authors selected galaxies to be star forming on the basis of emission lines in their optical spectra. The lines show the model predictions for the 1.4 GHz luminosity function in the rest frame. The model predictions are for z=0 (solid), 0.5 (dotted), 1 (dashed) and 2 (long dashed).

Fig. 6 shows the radio luminosity function for star forming galaxies. The data are from Sadler et al. (2002)[31], who combined the 2dFGRS and NVSS surveys to estimate the local luminosity function at 1.4GHz. Using the 2dFGRS spectra, galaxies were labelled as "star forming" or "active", depending on the emission lines displayed.

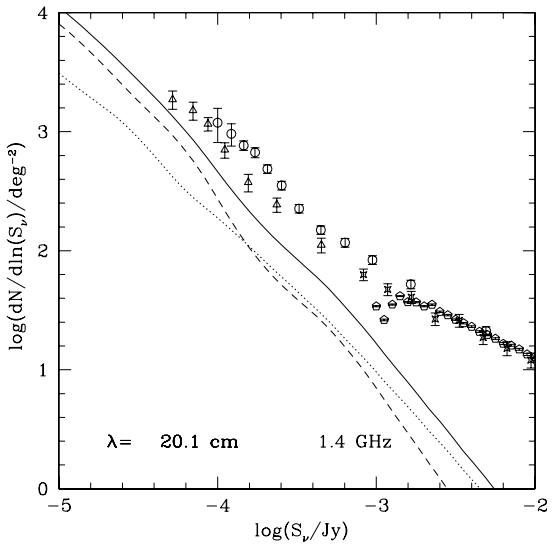


Figure 7. The radio source counts at 1.4GHz. The symbols show observational data: circles-Hopkins et al. (2003)[17], stars-Prandoni et al. (2001)[27], triangles-Richards (2000) [30], pentagons-White et al. (1997) [38]. Lines show the predictions for star forming galaxies; total (solid), bursts (dashed) and quiescent (dotted).

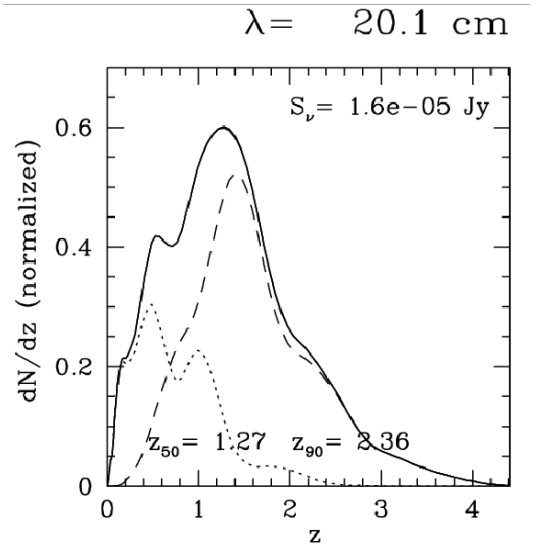


Figure 8. The predicted redshift distribution of normal star forming galaxies for a 1.4GHz flux of 16$\mu$Jy. The line styles are as in Fig. 7.

The active galaxies dominate the bright end of the radio luminosity function and are not shown in this plot. The model predictions at different redshifts are shown by the lines, as indicated in the caption. The luminosity function at a rest frame frequency of 1.4GHz shows a steady increase with redshift to $z \sim 2$, tracking the gradual increase in the global star formation rate in the model. The luminosity function declines somewhat after $z \sim 2$ as the star formation rate drops.

The number counts of sources at 1.4GHz are plotted in Fig. 7. In these data, no distinction is made between sources powered by star formation or accretion onto black holes. However, there is a clear change in the slope of the counts around 1mJy, suggesting that there is a shift in the dominant population responsible for the counts. The model predictions are shown by the curves, where we have divided the counts into starbursts and galaxies that are forming stars quiescently. The slope of the model counts is very similar to that of the faintest data points. The model is below the data, particularly at brighter fluxes, because we had not included the contribution of active radio galaxies in our predictions (the source counts due to AGN are discussed by Jarvis & Rawlings 2004[18]).

Finally, we present a prediction for the redshift distribution of faint radio sources in Fig. 8. These sources have a flux of 16$\mu$Jy, which is beyond the range of the current count data, but well within the reach of the SKA. The sources are predicted to be at a modest redshift, with a median of 1.3 and only 10% of the sources lying beyond $z \sim 2.4$. This is in contrast with SCUBA sources, for which the median redshift in both the observations and the models is $z \approx 2$ (Chapman et al. 2003 [7]; Baugh et al. 2004[1]).

## 6. Summary

We have argued that cosmic structures developed hierarchically and that models of galaxy formation should be set in this context. We have outlined a class of model, semi-analytical models of galaxy formation, that can follow the for-

mation and evolution of galaxies in a universe in which gravitational instability drives the formation of structure in the dark matter. Due to our poor knowledge of some aspects of the physics of galaxy formation, there is some uncertainty in how key ingredients, such as star formation and feedback, should be modelled. The model presented here is by no means unique and other models with different ingredients have also enjoyed some of the successes of our new model (e.g. Granato et al. 2004[14]). The appeal of semi-analytical modelling is its flexibility and speed. Different prescriptions for star formation can be plugged into the model and evaluated on the basis of the impact they have upon the predictions for the galaxy population. The SKA will have a huge influence upon the models, particularly on the physics of star formation, through measurements of the distribution of HI in the universe and the counts of faint, star forming radio sources.

## REFERENCES


1. Baugh C.M., Lacey C.G., Frenk C.S., Granato G.L., Silva L., Bressan A., Benson A.J., Cole S., 2004, MNRAS submitted, (astro-ph/0406069).
2. Benson A.J., Pearce F.R., Frenk C.S., Baugh C.M., Jenkins A., 2001, MNRAS, 320, 261.
3. Benson A.J., Lacey C.G., Baugh C.M., Cole S., Frenk C.S., 2002, MNRAS, 333, 156.
4. Benson A.J., Bower R.G., Frenk C.S., Lacey C.G., Baugh C.M., Cole S., 2003, ApJ, 599, 38.
5. Birnboim Y., Dekel A., 2003, MNRAS, 345, 349.
6. Bressan A., Silva L., Granato G.L., 2002, A&A, 392, 377.
7. Chapman S.C., Blain A.W., Ivison R.J., Smail I.R., 2003, Nature, 422, 695.
8. Cole S., Aragon-Salamanca A., Frenk C.S., Navarro J.F., Zepf S.E., 1994, MNRAS, 271, 781.
9. Cole S., Lacey C.G., Baugh C.M., Frenk C.S., 2000, MNRAS, 319, 168.
10. Condon J.J., Yin Q.F., 1990, ApJ, 357, 97.
11. Condon J.J., 1992, ARA&A, 30, 575.
12. Fukugita M., Hogan C.J., Peebles P.J.E., 1998, ApJ, 503, 518.
13. Granato G.L., Lacey C.G., Silva L., Bressan A., Baugh C.M., Cole S., Frenk C.S., 2000, ApJ, 542, 710.
14. Granato G.L., De Zotti G., Silva L., Bressan A., Danese L., 2004, ApJ, 600, 580.
15. Helly J.C., Cole S., Frenk C.S., Baugh C.M., Benson A., LaceyC., 2003a, MNRAS, 338, 903.
16. Helly J.C., Cole S., Frenk C.S., Baugh C.M., Benson A., LaceyC., Pearce F.R., 2003a, MNRAS, 338, 913.
17. Hopkins A.M., Afonso J., Chan B., Cram L.E., Georgakakis A., Mobasher B., 2003, AJ, 125, 465.
18. Jarvis M., Rawlings S., 2004, (this volume).
19. Jenkins A., Frenk C.S., White S.D.M., Colberg J.M., Cole S., Evrard A.E., Couchman H.M.P., Yoshida N., 2001, MNRAS, 321, 372.
20. Katz N., Keres D., Dave R., Weinberg D.H., 2002, to appear in the proceedings of 'The IGM/Galaxy Connection - the distribution of baryons at z=0'. (astro-ph/0209279).
21. Kauffmann G., White S.D.M., Guiderdoni B., 1993, MNRAS, 264, 201.
22. Keres D., Katz N., Weinberg D.H., Dave R., 2004, submittted to MNRAS. (astro-ph/0407095).
23. Keres D., Yun M.S., Young J.S., 2003, ApJ, 582, 659.
24. Okamoto T., Jenkins A., Eke V.R., Quilis V., Frenk C.S., 2003, MNRAS, 345, 429.
25. Peacock J.A., et al. (the 2dFGRS team), 2001, Nature, 410, 169.
26. Peroux C., McMahon R.G., Storrie-Lombardi L.J., Irwin M.J., 2003, MNRAS, 346, 1103.
27. Prandoni I., Gregorini L., Parma P., de Ruiter H.R., Vettolani G., Wieringa M.H., Ekers R.D., 2001, A&A, 365, 392.
28. Quilis V., 2004, MNRAS, 352, 1426, (astro-ph/0405389).
29. Rao S., Briggs F., 1993, ApJ, 419, 515.
30. Richards E.A., 2000, ApJ, 533, 611.
31. Sadler E.M., et al. (the 2dFGRS team), 2002, MNRAS, 329, 227.
32. Silva L., Granato G.L., Bressan A., Danese L., 1998, ApJ, 509, 103.
33. Somerville R.S., Primack J.R., 1999, MN-

RAS, 319, 1087.
34. Spergel D.N., et al. (the WMAP team), 2003, ApJS, 148, 175.
35. Storrie-Lombardi L.J., McMahon R.G., Irwin M.J., 1996, MNRAS, 283, L79.
36. Storrie-Lombardi L.J., Wolfe A.M., 2000, ApJ, 543, 552.
37. Sutherland R.S, Dopita M.A., 1993, ApJS, 88, 253.
38. White R.L., Becker R.H., Helfand D.J., Gregg M.D., 1997, ApJ, 475, 479.
39. Yoshida N., Stoehr F., Springel V., White S.D.M., 2002, MNRAS, 335, 762.
40. Zwaan M.A., Briggs F.H., Sprayberry D., Sorar E., 1997, ApJ, 490, 173.
41. Zwaan M.A., et al., 2003, AJ, 125, 2842.